SUPPLEMENTAL DATA

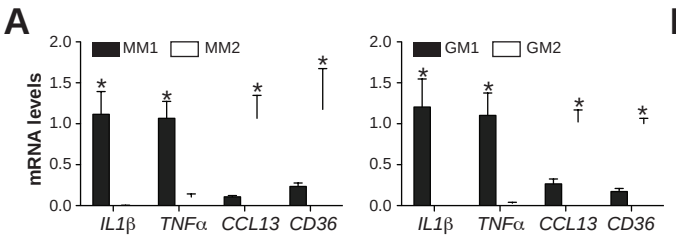

B

	Functional annotation	Targets	*p*-value
CC	membrane	192	$8x10^{-23}$
	plasma membrane	156	$3x10^{-15}$
	integral to plasma membrane	78	$1x10^{-7}$
BP	immune response	45	$1x10^{-7}$
	cell adhesion	45	$1x10^{-7}$
	antigen processing & presentation	18	$1x10^{-6}$

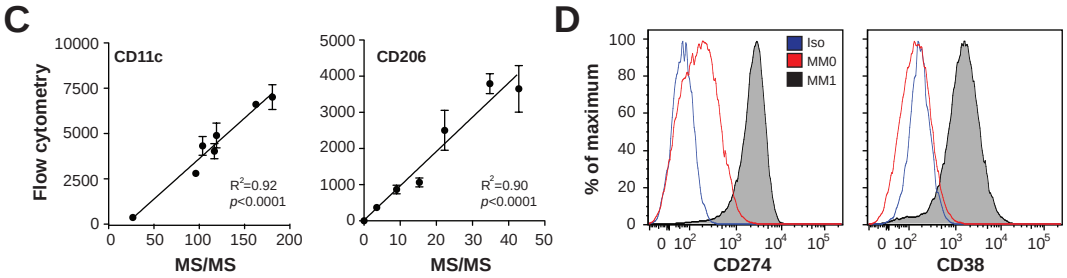

Fig. S1, related to Fig. 1. Analysis of human and murine polarized macrophages. *Panel A*: Polarization of human monocyte-derived macrophages differentiated with M-CSF or GM-CSF was confirmed by qRT-PCR using genes associated with M1 (*IL1β*, *TNFα*) and M2 macrophages (*CCL13*, *CD36*). *Panel B*: Functional annotation of cell surface proteins detected by mass spectrometry based on cellular component (CC) and biological process (BP). Statistical significance was assessed by the hypergeomtretic test with Benjamini-Hochberg correction. *Panel C*: Cell surface expression levels of CD11c and CD206 were quantified in the various cell types by flow cytometry (MFI) and mass spectrometry (MS/MS; spectral counts). Linear regression analyses demonstrated excellent concordance between the two methods. *Panel D*: Cell surface levels of CD274 and CD38 were quantified in murine MM0 and MM1 macrophages by flow cytometry. Where applicable, results are means and SEMs; *, denotes $p<0.05$, *t*-test.

A

Patient	Gender	Age	Genotype	FEV_1 (L)	Sputum microbiology
1	M	57	ΔF508/S945L	3.2 (68%)	*P. aeruginosa*
2	F	28	ΔF508/ΔF508	3.0 (76%)	*P. aeruginosa, M. avium*
3	M	27	ΔF508/ΔF508	3.6 (74%)	*S. aureus*
4	M	21	ΔF508/Q1330X	1.6 (44%)	*P. aeruginosa*
5	M	22	ΔF508/ΔF508	1.7 (50%)	*P. aeruginosa*

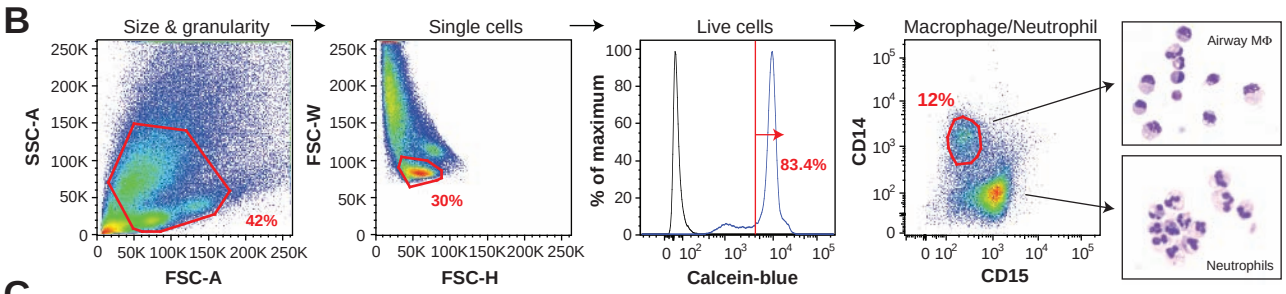

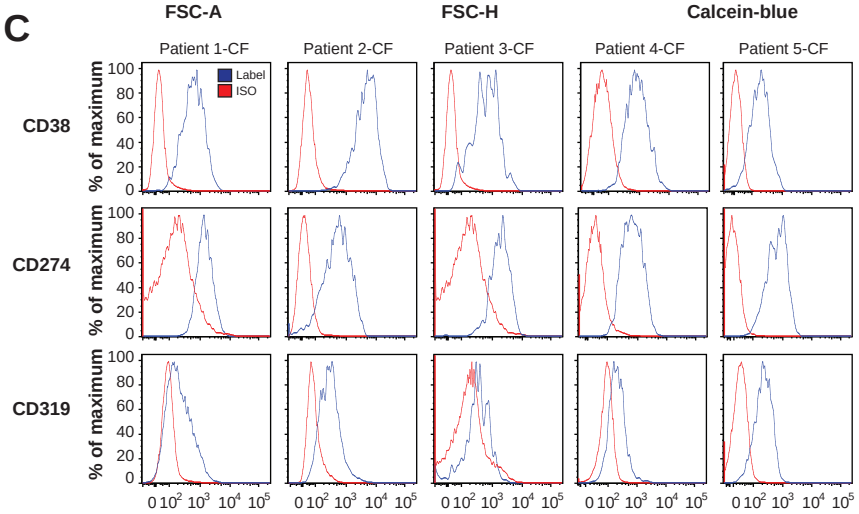

Fig. S2, related to Figs. 1,2. Flow cytometric analysis of airway macrophages from CF patients. *Panel A*: CF patient demographics. *Panel B*: Strategy for interrogating airway macrophage populations. Gates (red) represent cells that were selected for further analysis. Resultant airway macrophage populations, defined as CD14+CD15-, were confirmed by staining with Hema-3. *Panel C*: Cell surface levels of CD38, CD274, and CD319 on airway macrophages were assessed following the gating strategy shown in *Panel B*.

A

Group	N	Gender (F/M)	Age	BMI (kg/m^2)
Abdominoplasty	7	7/0	46.6+/- 3.3	26.2+/- 0.8
Bariatric surgery	7	5/2	48.6 +/- 3.5	40.4 +/- 2.6*

B

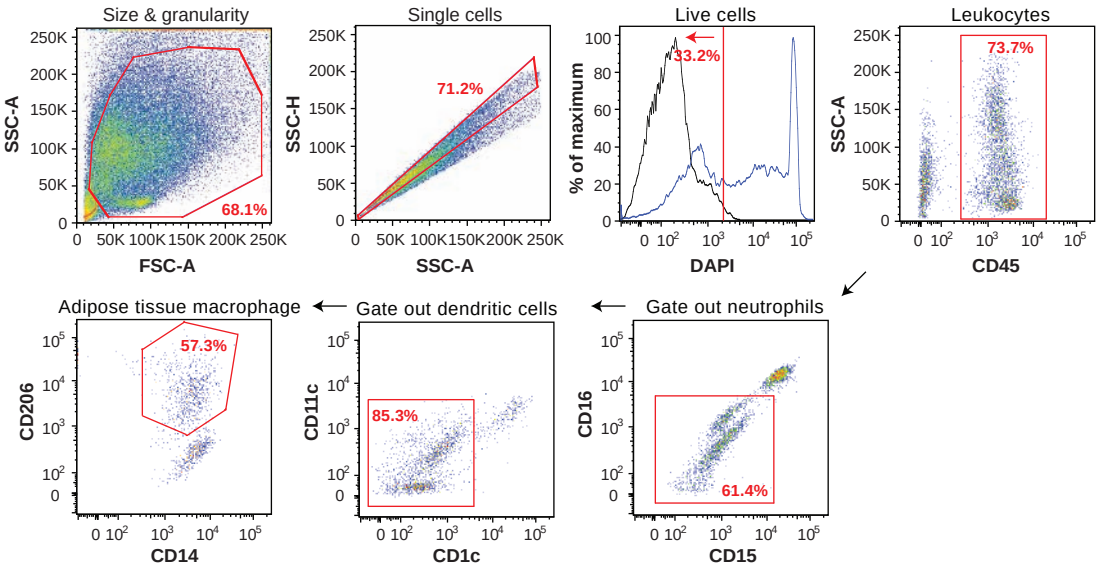

C

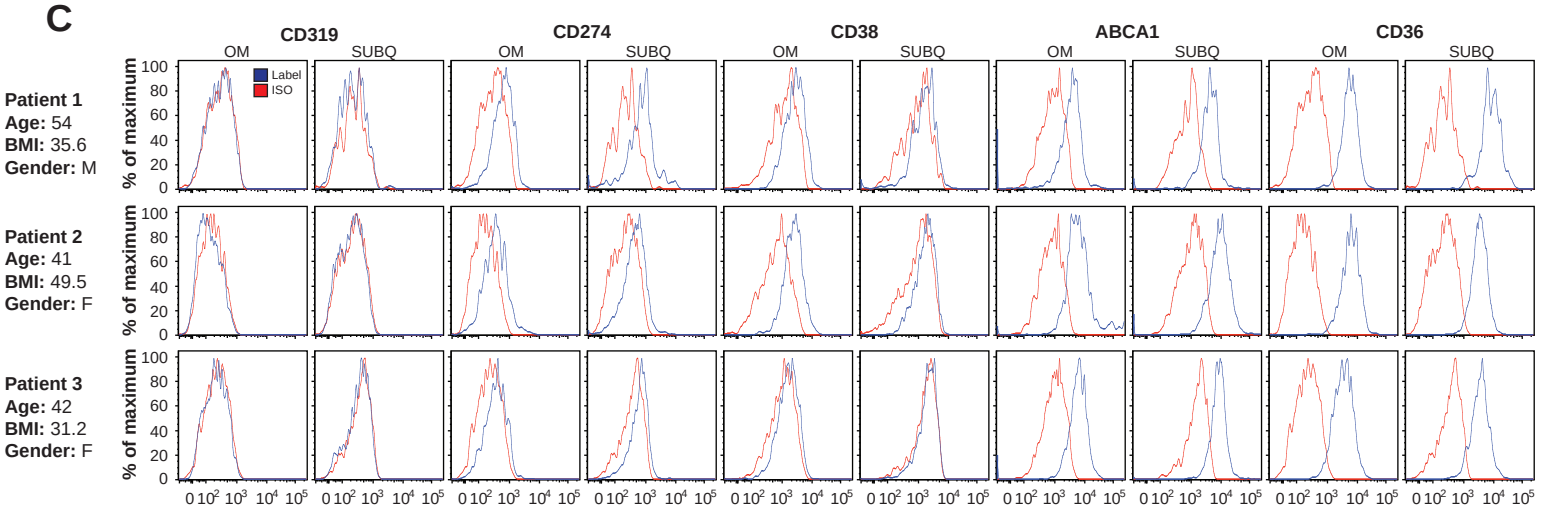

D

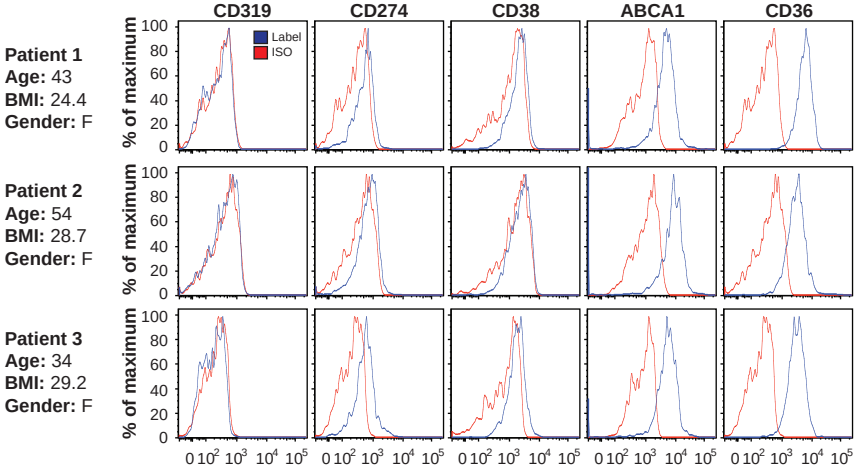

Fig. S3, related to Fig. 2. Flow cytometric analysis of ATMs from omental and subcutaneous fat. *Panel A*: Patient demographics. *Panel B*: Strategy for interrogating ATM populations. Gates (red) represent cells that were selected for further analysis. *Panels C-D*: Cell surface levels of CD38, CD274, CD319, ABCA1, and CD36 on ATMs isolated from omental (OM) or subcutaneous (SUBQ) adipose tissue collected from patients undergoing bariatric surgery (*Panel C*) or abdominoplasty (*Panel D*). For patients undergoing abdomnioplasty, analysis was performed with ATMs from subcutaneous adipose tissue. Data are provided for 3 representative patients using the gating strategy shown in *Panel B*.

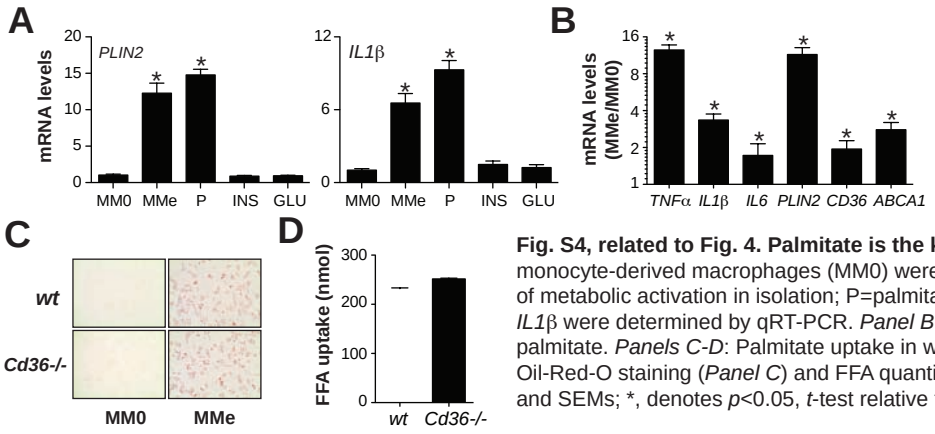

Fig. S4, related to Fig. 4. Palmitate is the key driver of metabolic activation. *Panel A*: Human monocyte-derived macrophages (MM0) were metabolically activated (MMe) or treated with components of metabolic activation in isolation; P=palmitate, INS=insulin, GLU=glucose. mRNA levels for *PLIN2* and *IL1β* were determined by qRT-PCR. *Panel B*: Human MM0 macrophages were treated with 0.1mM palmitate. *Panels C-D*: Palmitate uptake in wild-type and *Cd36-/-* murine BMDMs was assessed by Oil-Red-O staining (*Panel C*) and FFA quantification (*Panel D*). Where applicable, results are means and SEMs; *, denotes $p<0.05$, *t*-test relative to MM0.

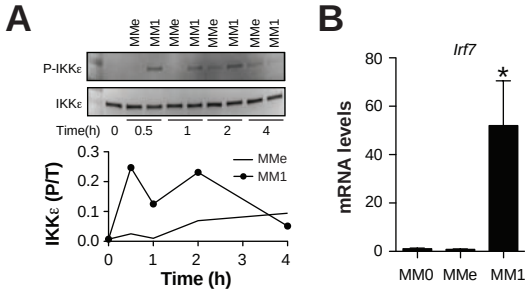

Fig. S5, related to Fig. 5. Murine MMe macrophages fail to activate the type I interferon response. Murine bone marrow-derived macrophages (MM0) were classically (MM1) or metabolically (MMe) activated. *Panel A*: Immunoblotting for total and phosphorylated (P-Ser172) IKKε. *Panel B*: *Irf7* mRNA levels. Where applicable, results are means and SEMs; *, denotes $p<0.05$, *t*-test relative to MM0.

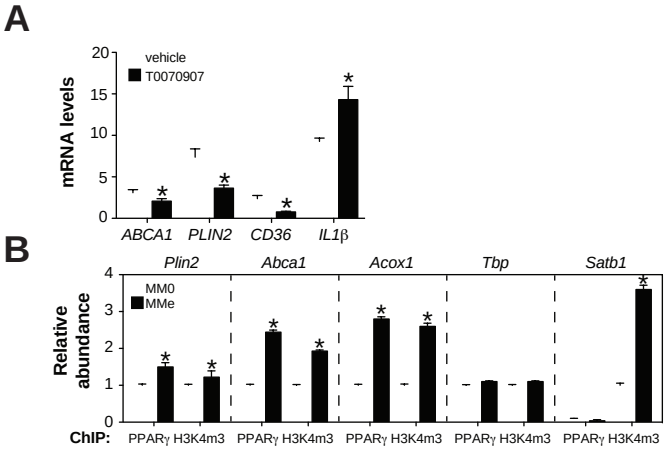

Fig. S6, related to Fig. 6. PPARγ regulates expression of MMe markers. *Panel A*: Gene expression in human MMe macrophages treated with a PPARγ antagonist (T0070907; 1μM). *Panel B*: Murine bone marrow-derived macrophages (MM0) were metabolically activated (MMe). PPARγ binding to its target and control gene promoters was assessed by ChIP analysis. Control genes were selected based on publically available ChIP-Seq data for PPARγ and RXR. Positive controls: *Acox1*, *Tbp1*; Negative control: *Satb1*. H3K4m3 ChIP was used as a marker for open chromatin. Results are means and SEMs; *, denotes $p<0.05$, *t*-test relative to control; N=4-6.

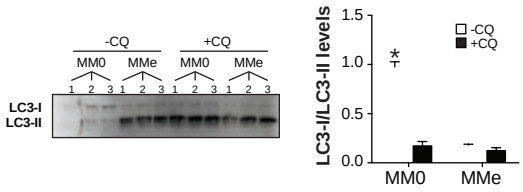

Fig. S7, related to Fig. 6. Metabolic activation inhbits autophagy. Human MM0 and MMe macrophages were treated wtih chloroquin (CQ; 100μM), an inhibitor of autophagy and LC3-I/-II levels were determined by immunoblotting. Where applicable, results are means and SEMs; *, denotes $p<0.05$, *t*-test.

SUPPLEMENTAL TABLE LEGENDS

Table S1, related to Fig. 1. Plasma membrane proteomics of human monocyte-derived macrophages. Proteomics analysis of classically activated (M1), alternatively activated (M2), and un-stimulated (M0) macrophages generated from human peripheral blood monocytes (Mn) in the presence of M-CSF (MM0, MM1, MM2) or GM-CSF (GM0, GM1, GM2). Proteins were quantified by spectral counting and differentially abundant proteins were identified using the *t*-test ($p < 0.05$) and *G*-test (*G*-statistic > 1.5).

Table S2, related to Fig. 3. Plasma membrane proteomics of classically and metabolically activated macrophages. Proteomics analysis of classically activated (M1), metabolically activated (MMe), and un-stimulated (M0) macrophages generated from human peripheral blood monocytes in the presence of M-CSF. Proteins were quantified by spectral counting and differentially abundant proteins were identified using the *t*-test ($p < 0.05$) and *G*-test (*G*-statistic > 1.5).

Table S3, related to Experimental Procedures. PCR primers used for PPARγ and H3K4m3 ChIP experiments. Sequences of human and murine PCR primers used in chromosome immunoprecipitation studies.

SUPPLEMENTAL EXPERIMENTAL PROCEDURES

Liquid chromatography-electrospray ionization-tandem mass spectrometry (LC-ESI-MS/MS) – Tryptic digests (1.5 µg) were loaded directly onto 2 cm C18 trap column (packed in-house), washed with 10 µl of solvent A (5% acetonitrile, 0.1% formic acid), and eluted on a 15 cm long, 75 µM reverse phase capillary column (ProteoPep™ II C18, 300 Å, 5 µm size, New Objective, Woburn MA). Peptides were separated at 300 nL/min over a 180 minute linear gradient from 5% to 35% buffer B (95% acetonitrile, 0.1% formic acid) on a Proxeon Easy n-LC II (Thermo Scientific, San Jose, CA). Mass spectra were acquired in the positive ion mode, using electrospray ionization and a linear ion trap mass spectrometer (LTQ Orbitrap Velos®, Thermo Scientific, San Jose, CA). The mass spectrometer was operated in data dependent mode, and for each MS1 precursor ion scan, the ten most intense ions were selected from fragmentation by CID (collision induced dissociation). Other parameters for mass spectrometry analysis included: resolution of MS1 was set at 60,000, normalized collision energy 35%, activation time 10ms, isolation width 1.5, and the +1 and +4 and higher charge states were rejected.

Peptide and protein identification – MS/MS spectra were searched against the International Protein Index (Kersey et al., 2004) human (v3.87, 91464 entries) primary sequence database using Sorcerer™-SEQUEST® (version v. 3.5,) (Sage-N Research, Milpitas, CA). Search parameters included semi-enzyme digest with trypsin (after Arg or Lys) with up to 2 missed cleavages. SEQUEST® was searched with a parent ion tolerance of 50 ppm and a fragment ion mass tolerance of 1 amu with fixed Cys alkylation, and variable Met oxidation. SEQUEST results were further validated with PeptideProphet (Keller et al., 2002) and ProteinProphet (Nesvizhskii et al., 2003) using an adjusted probability of ≥0.90 for peptides and ≥0.96 for proteins. Proteins considered for analysis had to be identified in at least 5 of 6 replicates for one biological condition.

Protein quantification and statistical analysis – Proteins detected by LC-MS/MS were quantified by spectral counting, the total number of MS/MS spectra detected for a protein (Liu et al., 2004). Differences in relative protein abundance were assessed with

the *t*-test and *G*-test (Becker et al., 2010). Permutation analysis was used to empirically estimate the FDR. Significance cutoff values for the *G*-statistic and *t*-test were determined using PepC (Heinecke et al., 2010).

qRT-PCR – Relative quantification of PCR products was based on value differences between the target and 18S control, using the $2^{-\Delta\Delta Ct}$ method (Livak and Schmittgen, 2001). To normalize whole adipose tissue cytokine measurements to the number of ATMs in the tissue, data were further standardized to CD206 (a general marker of human ATMs; (Zeyda et al., 2007)) expression levels.

Chromatin Immunoprecipitation – ChIP experiments were performed as previously described (Mutskov et al., 2002). Briefly, samples were cross-linked with 1% formaldehyde, sheared to obtain chromatin fragments ranging in size from 200 to 500 bp, and immunoprecipitated with antibodies specific for PPARγ (Santa Cruz Biotechnology Inc.; sc-7196) or histone H3K4m3 (Millipore; 07-473). Purified input and immunoprecipitated DNA were amplified and analyzed by Q-PCR using specific primers (**Table S3**) at the region of interest. ChIP data analyses were performed as previously described (Mutskov and Felsenfeld, 2004). Fold difference of a target sequence (t) in the IP fraction versus a fixed amount of input (In) DNA was calculated according to $IP/In = 2^{-\Delta\Delta Ct} = 2^{-(Ct(IP)-Ct(In))}$. Primers were designed based on previously published PPARγ ChIP-Seq data (Mikkelsen et al., 2010) and the RXR-binding sites from the ENCODE project. For each primer set, fold difference values were corrected by subtraction of the nonspecific signal derived from the nonimmune rabbit IgG ChIP (t0), where $(IP/In)^{t} - (IP/In)^{t0}$. In parallel, DNA samples were amplified with primers for an internal control primer (c), and the relative abundance of target sequences to the internal control sequence was calculated using the following formula: $[(IP/In)^{t} - (IP/In)^{t0}] / [(IP/In)^{c} - (IP/In)^{c0}]$.

SUPPLEMENTAL REFERENCES

Heinecke, N.L., Pratt, B.S., Vaisar, T., and Becker, L. (2010). PepC: proteomics software for identifying differentially expressed proteins based on spectral counting. Bioinformatics *26*, 1574-1575.

Keller, A., Nesvizhskii, A.I., Kolker, E., and Aebersold, R. (2002). Empirical statistical model to estimate the accuracy of peptide identifications made by MS/MS and database search. Anal Chem *74*, 5383-5392.

Kersey, P.J., Duarte, J., Williams, A., Karavidopoulou, Y., Birney, E., and Apweiler, R. (2004). The International Protein Index: an integrated database for proteomics experiments. Proteomics *4*, 1985-1988.

Liu, H., Sadygov, R.G., and Yates, J.R., 3rd (2004). A model for random sampling and estimation of relative protein abundance in shotgun proteomics. Anal Chem *76*, 4193-4201.

Livak, K.J., and Schmittgen, T.D. (2001). Analysis of relative gene expression data using real-time quantitative PCR and the 2(-Delta Delta C(T)) Method. Methods *25*, 402-408.

Mutskov, V., and Felsenfeld, G. (2004). Silencing of transgene transcription precedes methylation of promoter DNA and histone H3 lysine 9. The EMBO journal *23*, 138-149.

Mutskov, V.J., Farrell, C.M., Wade, P.A., Wolffe, A.P., and Felsenfeld, G. (2002). The barrier function of an insulator couples high histone acetylation levels with specific protection of promoter DNA from methylation. Genes & development *16*, 1540-1554.

Nesvizhskii, A.I., Keller, A., Kolker, E., and Aebersold, R. (2003). A statistical model for identifying proteins by tandem mass spectrometry. Anal Chem *75*, 4646-4658.

Zeyda, M., Farmer, D., Todoric, J., Aszmann, O., Speiser, M., Gyori, G., Zlabinger, G.J., and Stulnig, T.M. (2007). Human adipose tissue macrophages are of an anti-inflammatory phenotype but capable of excessive pro-inflammatory mediator production. Int J Obes (Lond) *31*, 1420-1428.